出國報告（出國類別：國際會議）

主動式孤島偵測法結合智慧型控制器

服務機關：國防大學理工學院電機電子系
姓名職稱：中校教師藍建武
派赴國家：日本
出國期間：105/05/25-105/05/29
報告日期：105/06/21

摘要

本次公務出國之目的為參加由世界科學、工程與技術學院 (World Academy of Science, Engineering and Technology, WASET)於日本東京成田東武機場酒店(Narita Tobu Hotel Airport)所舉辦的 2016 年「第 18 屆電機工程與技術國際研討會」(18th International Conference on Electrical Engineering and Technology, ICEET 2016)並發表論文，論文題目為「主動式孤島偵測法結合智慧型控制器」(Active Islanding Detection Method Using Intelligent Controller)，論文內容主要說明利用直流源換流器模擬分散式發電系統來執行實、虛功率之追蹤控制與孤島偵測，並利用兩個機率模糊類神經網路(PFNN)智慧型控制器來取代傳統比例積分(PI)控制器。該篇論文於日前投稿本次研討會時榮獲刊登，並安排於 105 年 5 月 27 日上午 10:45 至 13:00 之場次進行電子海報發表。本次研討會發表行程於 105 年 5 月 25 日出發，並於 105 年 5 月 29 日完成任務順利返國。

目次

頁次

壹、目的：

為持續拓展自身研究能量與累積研究績效，因此選擇參加本次由世界科學、工程與技術學院所舉辦的 2016 年「第 18 屆電機工程與技術國際研討會」，本次研討會所發表的內容主要是與本院電機機械實驗室所共同合作的研究成果，內容在說明如何利用直流源換流器模擬分散式發電系統來執行實、虛功率之追蹤控制與孤島偵測，並利用兩個機率模糊類神經網路(PFNN)智慧型控制器來取代傳統比例積分(PI)控制器。藉由本次國際型研討會的發表，希望能為提升國軍國防科技之學術地位略盡棉薄之力。

貳、過程：

本次參加研討會行程出發當日搭乘 04:25 自桃園機場二航廈起飛之中華航空，預計在日本當地時間 08:25 時抵達東京成田機場二航廈，本次班機準時抵達目的地，在購買本次行程所需之交通票卷後，選擇搭程京城電鐵公司的 Skyliner 快速地鐵前往上野，車程約 40 分鐘，並以步行方式前往下榻之 APA 飯店上野站前分店。由於抵達時尚無法辦理入住，因此僅能先於寄放行李後，選擇在附近的餐館用餐並稍事休息。由於東京交通方式複雜，因此當天行程主要在了解飯店周圍主要車站地點及搭車方式，當晚便在飯店休息及了解研討會相關議程。

研討會第一天，由於研討會場地位於成田機場附近的成田東武飯店，因此我們便搭乘京城電鐵公司的 Skyliner 快速地鐵返回成田機場，再搭乘計程車前往會場，約 10 時許抵達並完成報到手續。會場共有 A、B 兩個議程同時進行，由於我們所發表的論文表訂於 27 日進行發表，因此當日報到完成後便挑選幾場較感興趣的場次進行聆聽，以下簡單摘述較能理解的發表內容。首先是由 Tajik National University 所發表的「The Impact of Water Reservoirs on Biodiversity and Food Security and the Creation of Adaptation Mechanisms」，內容在說明如何考慮大型水庫的興建位置與施工條件，以對引起的環境及氣候變化帶來最小的影響，並以農田灌溉所需水量來進行評估。接著，是由日本 Kyushu University 所發表的「Quantitative Analysis of Nutrient Inflow from River and Groundwater to Imazu Bay in Fukuoka, Japan」，說明日本今津灣長是瀕危物種培育的重要場所，但由於該區域為半封閉海灣，水體交換緩慢導致優養化嚴重，因此該研究透過分析 TN、TP、NO3-N 及 NH4-N 負荷量來評估今津灣的優養化程度。在下午的場次，則聆聽由 Cochin University of Science and Technology 所發表的「Investigation into Black Oxide Coating of 410 Grade Surgical Stainless Steel Using Alkaline Bath Treatment」，由於醫療級不鏽鋼手術器材的高反射率，容易導致腹腔手術時受到器材反射光線的設備精度失控，該研究提出如何製作適用於醫療等級的黑色氧化物及鍍膜技術，以提升在精密手術時的視覺清晰度。

在研討會第二天，也是我們本次投稿發表的場次，當日約 9 時許抵達會場，我們所發表的「Active Islanding Detection Method Using Intelligent Controller」預定於 10:45 至 13:00 的場次進行發表，內容說明如何利用輸入干擾訊號，並結合智慧型控制器以達到孤島偵測之目的。當日其他學者所發表的研究內容摘述如下。首先，在 08:00 至 10:30 場次所聆聽的論文是由 King Mongkut’s University of Technology Thonburi 所發表的「A Prediction Method for Large-Size Event Occurrences in the Sandpile Model」，該研究藉由考慮 Bak-Tang-Wiesenfeld 的沙堆模型來實現對大型事件的預測機制，並對時間序列進行分析，最後證明此種方式比起隨機預測來的更有效率。接著，是由 Pukyong National University 所發表的「Quantile Coherence Analysis: Application to Precipitation Data」，提出位數相關分析法來對兩組數據於線性非時變關係相關分析。由於傳統相關分析著重於分析均值關係，導致對異常值過於敏感而影響分析結果，該研究利用拉普拉斯交叉週期圖的一般版本，建立兩組數據之廣義交叉週期圖至位數交叉週期圖，並提供兩組數據間更豐富的相

互關係。該研究並提出真實數據為例，以證明位數相關分析法的有效性。在 Hacettepe University 所發表的「$\bar{X}$ and S Control Charts based on Weighted Standard Deviation Method」論文中，提出基於正態假設的 Shewhart 圖由於 Type-I 錯誤率膨脹，並不適用於偏態分布，因此該研究提出觀察加權標準差與 S 因子控制圖的方法來估算偏態分布的過程變化，此方法不僅簡單，且容易計算，更可依據偏斜的方向與角度來建構非對稱的上下限。該研究並透過模擬分析來證明在大樣本下的良好性能。在我們論文發表的同個場次，亦聆聽了 National Institute of Technology, Nara College 所發表的「Metal Berthelot Tubes with Windows for Observing Cavitation under Static Negative Pressure」，由於在負壓下不易去除氣穴，因此本研究提出了將金屬 Berthelot 管建置於觀察窗的方法，來了解是否產生高度的負壓環境。藉由觀察負壓產生的趨勢，即可作為避免空穴產生的手段。

在經過連日的行程，最後乙日上午於飯店充分休息後，於下午 1 時許搭乘京城電鐵公司的 Skyliner 快速地鐵返回成田機場辦理相關手續，並搭乘當地 18:30 起飛之中華航空班機，於晚間 21:00 返回國門，順利完成本次日本國際研討會論文發表行程。

參、心得及建議：

參加日本東京研討會是件難得的經驗，高度的自動化與錯縱複雜的地鐵建構起繁榮的都市，但也隨處可見高度競爭生活下的殘酷面，例如一早至 24 小時營業的速食店用早餐時，隨處可見西裝筆挺，但看起來徹夜未眠的上班族蜷伏在店家角落的座位打盹；而到了夜晚，車站的聯絡道更四處可見搭起紙箱，且仍不忘形象而整齊排列的街友露宿街頭，這樣的畫面令人不寒而慄。而語言的隔閡也是一大考驗，雖然日文中仍有部分漢字可供辨識；機場及飯店等地尚可使用英語溝通，但大部分生活區的日本人是無法使用英語溝通的！更令人印象深刻的是複雜的地鐵，由於日本有區分公鐵與私鐵，且又區分為不同的路線圖，加上車站彼此可能並未相連，因此在語言隔閡的狀況下，如何搭車前往目的地變成了一項嚴峻的挑戰，若要改搭計程車，不僅價格高昂，且如何與司機溝通目的地亦讓人卻步。所幸目前東京已針對各家的 IC 卡通路進行整合，類似台灣的悠遊卡，無論是哪一條鐵路路線，只要進出站感應磁卡即可搭乘，若餘額不足再找尋車站內可顯示多國語言的精算機進行儲值即可，對於避免掉比手畫腳的溝通方式可真是幫了我們不少大忙。因此，對於未來需要前往東京參加研討會的同仁，建議務必要先對當地所要搭乘的交通工具作好功課再前往，以免面對錯縱複雜的交通方式而耽誤了行程。

最後，也感謝各級同仁在繁瑣的行政程序中所給予的各項熱心協助，更感謝科技部所提供寶貴經費，才能讓這次的發表行程順利成行，未來將持續努力的累積研究能量，以期能為本國的學術領域貢獻一份心力！

肆、參考資料：

補充參加研討會所記錄之場地及議程照片。

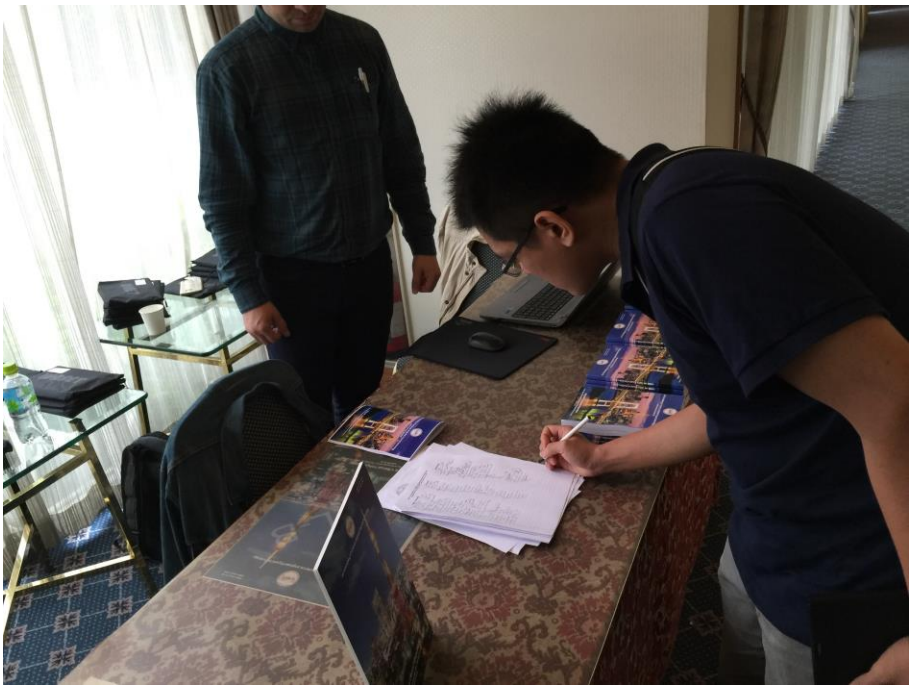

研討會簽到

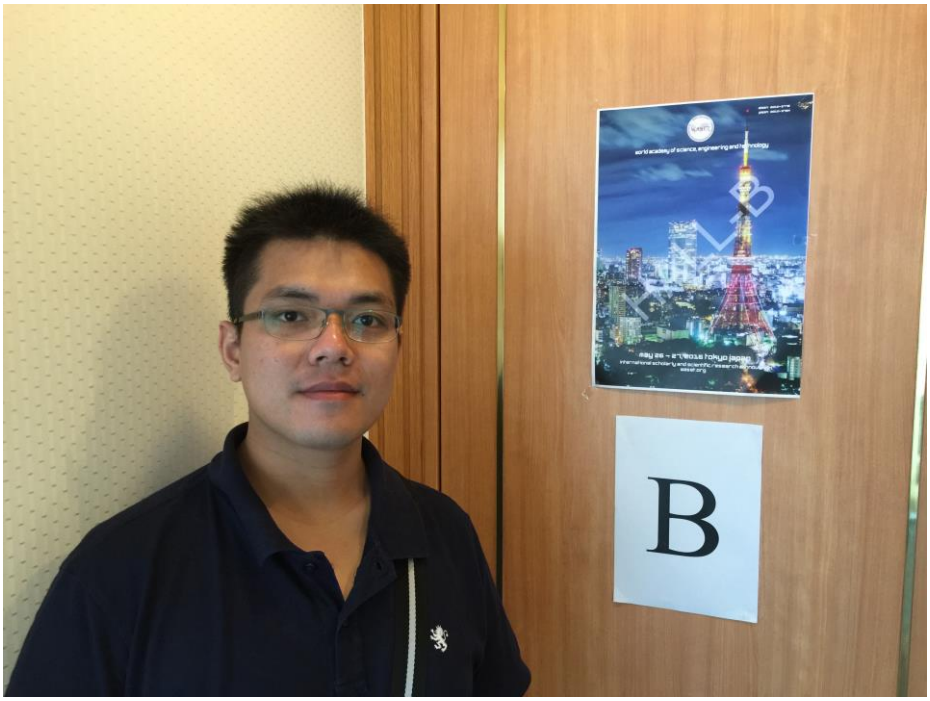

研討會報告場地

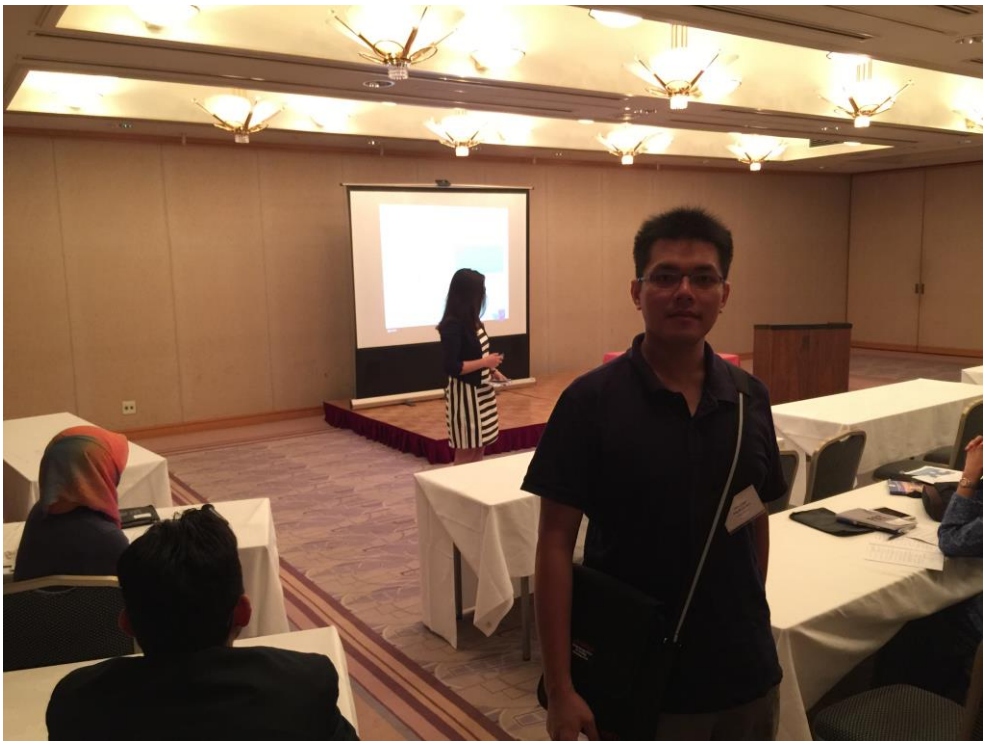

研討會會議進行(1)

研討會會議進行(2)

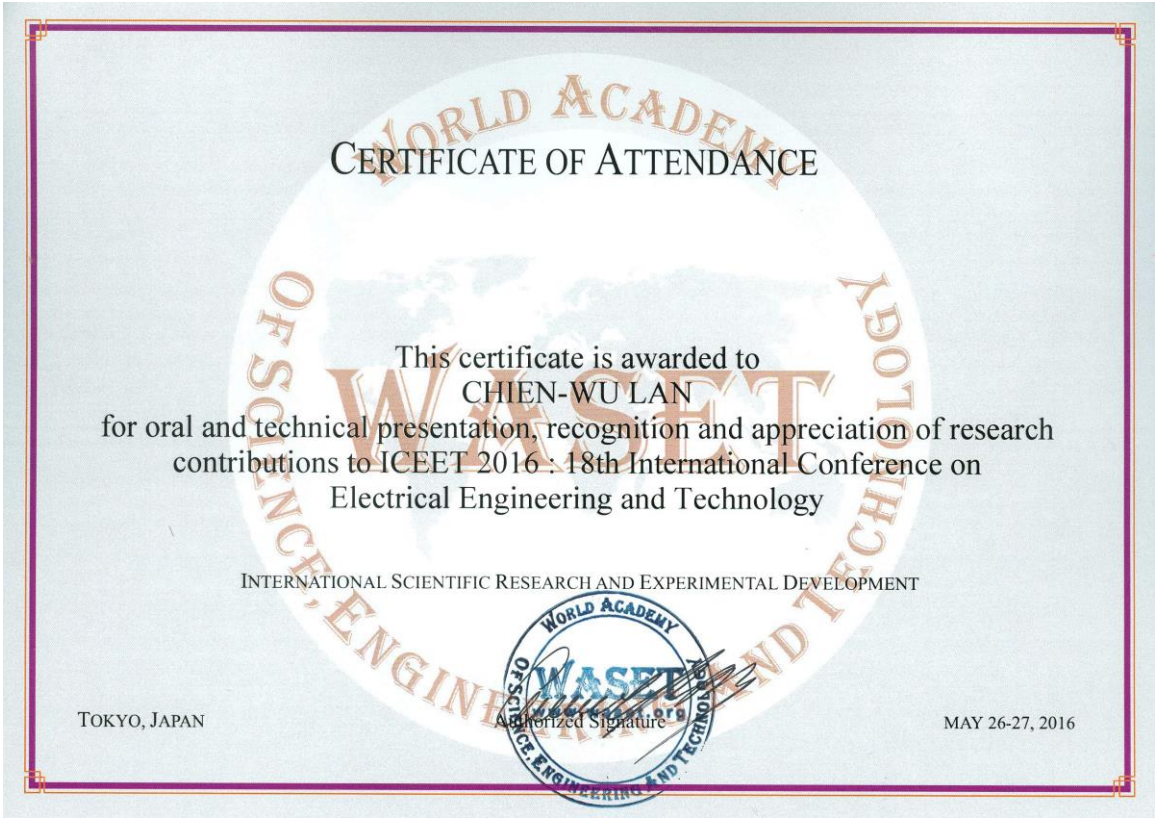

CERTIFICATE OF ATTENDANCE

This certificate is awarded to
CHIEN-WU LAN
for oral and technical presentation, recognition and appreciation of research contributions to ICEET 2016 : 18th International Conference on Electrical Engineering and Technology

INTERNATIONAL SCIENTIFIC RESEARCH AND EXPERIMENTAL DEVELOPMENT

TOKYO, JAPAN

Authorized Signature

MAY 26-27, 2016

出席證明

伍、會議資料：

（收錄於論文集光碟片，論文集第 3722 至 3728 頁）

Active Islanding Detection Method Using Intelligent Controller

Kuang-Hsiung Tan, Chih-Chan Hu, Chien-Wu Lan, Shih-Sung Lin, Te-Jen Chang

***Abstract*—**An active islanding detection method using disturbance signal injection with intelligent controller is proposed in this study. First, a DC\AC power inverter is emulated in the distributed generator (DG) system to implement the tracking control of active power, reactive power outputs and the islanding detection. The proposed active islanding detection method is based on injecting a disturbance signal into the power inverter system through the *d*-axis current which leads to a frequency deviation at the terminal of the *RLC* load when the utility power is disconnected. Moreover, in order to improve the transient and steady-state responses of the active power and reactive power outputs of the power inverter, and to further improve the performance of the islanding detection method, two probabilistic fuzzy neural networks (PFNN) are adopted to replace the traditional proportional-integral (PI) controllers for the tracking control and the islanding detection. Furthermore, the network structure and the online learning algorithm of the PFNN are introduced in detail. Finally, the feasibility and effectiveness of the tracking control and the proposed active islanding detection method are verified with experimental results.

***Keywords*—**Distributed generators, probabilistic fuzzy neural network, islanding detection, non-detection zone.

I. Introduction

ISLANDING detection is an essential protection requirement for distributed generators (DGs) for personnel and equipment safety. The islanding phenomenon for the DG is defined when the DG continues to operate with local loads when the utility power is disconnected [1]. The islanding phenomenon usually occurs when the load power and the output power of the DG are balanced, i.e., the load power is entirely supplied by the DG. At this time, if the utility power is failed or interrupted, the disturbances of frequency and voltage of the DGs cannot be detected with the standard of IEEE1547or UL1741 [2], [3]. The islanding phenomenon will damage the power systems and the safety of maintenance staffs. Thus, all DG equipment is required to present an effective islanding detection method [4].

In the past decade, many literatures [5]-[8] have been proposed to prevent islanding phenomenon caused by DGs. In [5], the active frequency drift method was proposed to add dead time into the output current of the power inverter and resulted in current and voltage distortion at the point of common coupling (PCC). Thus, when the utility power is failed or interrupted, the frequency can drift beyond the non-detection zone (NDZ). In [6], the proposed active islanding detection method is based on injecting a negative-sequence current through the power inverter by means of unified three-phase signal processor. The signal cross-correlation index between the injected reactive power and the frequency deviation at the PCC is proposed to detect the islanding phenomenon in [7]. A positive feedback anti-islanding scheme using *q*-axis injection method was proposed. The method injects a disturbance signal, which contains the difference of terminal voltage, into the active power axis (*q*-axis). When the utility power is failed or interrupted, it can accelerate the voltage to drift beyond the NDZ [8]. However, the proposed method is based on the active power disturbance method for islanding detection which inherently has larger NDZ compared with the reactive power disturbance method for islanding detection [9].

Recently, the study about the integration of artificial neural network and fuzzy has been proposed in many research fields. The fuzzy neural network (FNN) owns the abilities of prediction, modeling, training, and solving problems with uncertainty [10]. Moreover, FNN does not require mathematical models and has the ability to approximate nonlinear systems [11]. Furthermore, nowadays, the new intelligent controllers, probabilistic neural network (PNNs), have also been proposed in the literatures [12]-[15]. The PNN is a feed-forward neural network and is a direct neural network implementation of Bayes classification rule and Parzen nonparametric probability density function (PDF) estimation [12]. In addition, the PNN has an inherent parallel structure, a fast training process, and guaranteed optimal classification performance if a sufficiently large training set is provided [13]. Therefore, the PNN can handle the uncertainties in industry applications effectively, and it has been widely used in nonlinear mapping, pattern classification, and classification and fault detection [14], [15]. Owing to the above advantages of PNN and FNN, the PFNN, which integrates the characteristics of PNN and FNN, has been proposed in some applications, such as stochastic modeling and control problems. In [16], the PFNN is capable of solving the uncertainties in industry applications.

In this study, a grid-connected three-phase DG system using the adopted PFNN controllers is researched for the tracking control and the islanding detection. First, a DC source power inverter is emulated the DG system to implement the tracking control of active power, reactive power outputs and the

C. C. Hu is with System Manufacturing Center, National Chung-Shan Institute of Science and Technology, Sanxia District, New Taipei City 23742, Taiwan (e-mail: huchihchan@gmail.com).

K. H. Tan is with the Department of Electrical and Electronic Engineering, Chung Cheng Institute of Technology, National Defense University, Taoyuan 335, Taiwan (corresponding author; phone: +886-3-380-9991 ext.128; e-mail: s913115@gmail.com).

C. W. Lan, S. S Lin and T. J. Chang are with the Department of Electrical and Electronic Engineering, Chung Cheng Institute of Technology, National Defense University, Taoyuan 335, Taiwan (e-mail: g941339@gmail.com; shihsunglin@gmail.com; karl591218@gmail.com).

islanding detection. Then, the characteristics of the NDZ and the proposed active islanding detection method using disturbance signal injection are introduced in detail. Moreover, the PFNNs are adopted to replace the traditional PI controllers for the tracking control and the islanding detection to improve the transient and steady-state responses of the active power and reactive power outputs of the power inverter, and the performance of the islanding detection method. Furthermore, the training algorithm based on backpropagation (BP) is derived to train the connective weights, means, and standard deviations of the membership functions in the adopted PFNN online. Finally, the adopted PFNN controllers to control the active power and reactive power outputs of the power inverter and to detect the islanding phenomenon is realized in a personal computer (PC)-based control computer via MATLAB & Simulink, and the effectiveness is verified by experimentation.

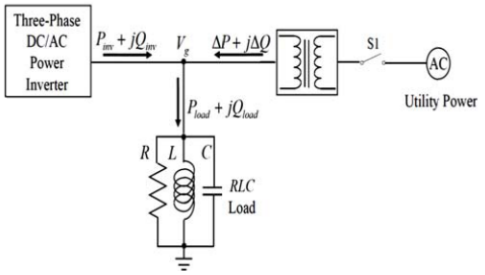

Fig. 1 Test circuit with parallel RLC load

II. Active Islanding Detection Method

A. Non-Detection Zone

The NDZ is derived from the test circuit with a parallel *RLC* resonant tank as the load as shown in Fig 1. The power flow relations of the inverter active power P_{inv}, reactive power Q_{inv}, *RLC* load active power P_{load}, reactive power Q_{load}, and utility active power ΔP, reactive power ΔQ are as follows:

$$P_{inv} = P_{load} - \Delta P;\ Q_{inv} = Q_{load} - \Delta Q. \tag{1}$$

It is difficult to detect the islanding phenomenon when active power and reactive power outputs of the grid-connected power inverter are equal to the active and reactive power of the *RLC* load, i.e., $\Delta P = 0$, $\Delta Q = 0$ [17]. When the utility power is disconnected, the added disturbance signal in the *d*-axis current will result in $Q_{inv} \neq 0$. It can be obtained as;

$$Q_{inv} = V_g^2(\frac{1}{\omega_g L} - \omega_g C) = P_{load} R(\frac{1}{\omega_g L} - \omega_g C), \tag{2}$$

where ω_g is the angular frequency of the utility power; V_g is the terminal *rms* voltage of *RLC* load. Moreover, the quality factor is defined as;

$$Q_f = R\sqrt{\frac{C}{L}} \tag{3}$$

Substitute (3) into (2), then (2) can be rewritten as follows:

$$\frac{Q_{inv}}{P_{load}} = Q_f(\frac{1}{\omega_g\sqrt{LC}} - \omega_g\sqrt{LC}). \tag{4}$$

Since the resonant frequency ω_o equals $\sqrt{1/LC}$, (4) can be rewritten as follows:

$$\frac{Q_{inv}}{P_{load}} = Q_f(\frac{\omega_o}{\omega_g} - \frac{\omega_g}{\omega_o}) = Q_f(\frac{f_o}{f_g} - \frac{f_g}{f_o}), \tag{5}$$

where f_g and f_o are the frequency of ω_g and ω_o. The NDZ is obtained with the maximum and minimum frequency defined in the IEEE Standard 1547 [2] as follows:

$$Q_f(\frac{f_{min}}{f_g} - \frac{f_g}{f_{min}}) \le \frac{Q_{inv}}{P_{load}} \le Q_f(\frac{f_{max}}{f_g} - \frac{f_g}{f_{max}}), \tag{6}$$

where $f_{\max}$ and f_{min} are the maximum and minimum frequency thresholds; $Q_f(\frac{f_{min}}{f_g} - \frac{f_g}{f_{min}})$ is the lower limit of the NDZ; $Q_f(\frac{f_{max}}{f_g} - \frac{f_g}{f_{max}})$ is the upper limit of NDZ.

B. Active Islanding Detection Method Using Disturbance Signal Injection

The proposed active islanding detection method is based on injecting a disturbance signal into the power inverter system through the *d*-axis current as shown in Fig. 2, where P_{inv}^* is the active power command of the power inverter; Q_{inv}^* is the reactive power command of the power inverter; θ is the synchronous angle obtained by phase loop lock (PLL); i_{de}^* and i_{qe}^* are the *d*-*q* axes current commands; i_{us}^*, i_{vs}^*, i_{us}^* are three-phase current commands. The errors of active power and reactive power are regulated by the PI or PFNN controllers to obtain the *d*-*q* axes current commands. Then, using the coordinate transformation algorithm, three-phase current commands can be generated. The *d*-axis current command i_{de}^* consists of *d*-axis current i_{de} and injected disturbance signal i_{dist}. The magnitude of the injected disturbance signal i_{dist} becomes stronger when the utility power is disconnected. The injected disturbance signal i_{dist} is designed as:

$$i_{dist} = k\,sign(\Delta f),\ sign(\Delta f) = \begin{Bmatrix} 1, & f[k] > f[k-1] \\ 0, & f[k] = f[k-1] \\ -1, & f[k] < f[k-1] \end{Bmatrix} \tag{7}$$

where k is the gain of disturbance signal; *sign* is the sign function, and $sign(\Delta f)$ is determined by the frequency difference of current and last samples.

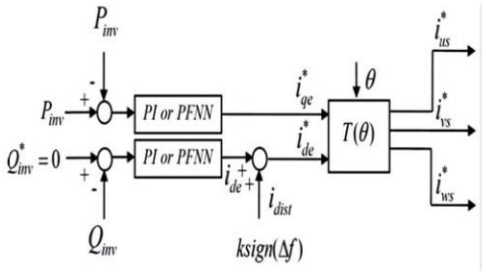

Fig. 2 Control block of proposed islanding detection method

The proposed active islanding detection method can push the frequency of the power inverter f to drift beyond the NDZ by adding the disturbance signal i_{dist} in the *d*-axis current i_{de} when the utility power is disconnected.

III. Probabilistic Fuzzy Neural Network Controller

Though the PI control has the advantages of simple structure and is easily implemented, the traditional PI controller is not robust in dealing with system uncertainties such as modeling errors, parameter variations and external disturbances in practical applications. Hence, in order to achieve superior effect for the proposed active islanding detection method, the online trained PFNN controllers are adopted to replace the traditional PI controllers to achieve further rapid response of the islanding detection and improve the transient and steady-state responses of the active power and reactive power outputs of the power inverter.

A. Network Structure

The adopted five-layer of the PFNN is illustrated in Fig. 3, which consists of the input layer, the membership layer, the probabilistic layer, the rule layer and the output layer. Moreover, the signal propagation and the basic function of each layer are described in detail as follows:

1. Input layer (layer 1): For every node in this layer, the node input and the node output are obtained as:

$$x_i(N) = e_i(N), \quad i = 1, 2 \tag{8}$$

where x_i represents the *i*th input to the input layer; *N* represents the *N*th iteration. The inputs of the PFNN are $e_1(N) = e$ and $e_2(N) = \dot{e}$, which are the tracking error and its derivative, respectively. These nodes only pass the input signal to the next layer. In this study, the input variables are $e = P^*_{inv} - P_{inv}$ for the active power control and $e = Q^*_{inv} - Q_{inv}$ for the reactive power control.

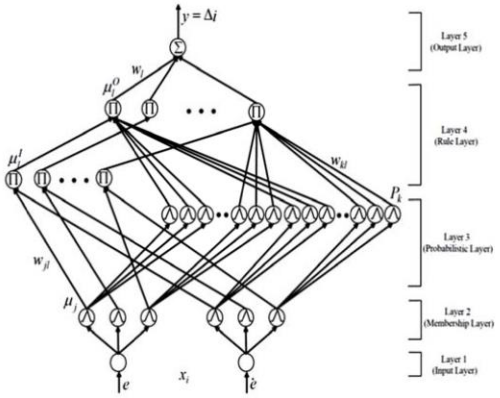

Fig. 3 Network structure of PFNN

2. Membership layer (layer 2): In this layer, the receptive field function is usually a Gaussian function in FNN. In order to reduce the computational requirements, a triangular function $f_m(x_i)$ is selected as the receptive field function. The equations of the triangular function $f_m(x_i)$ are provided as:

$$\mu_j(x_i) = f_m(x_i) = \begin{cases} 0 & if \quad x_i \ge m_j + \sigma_j,\ x_i \le m_j - \sigma_j \\ \dfrac{x_i - m_j + \sigma_j}{\sigma_j} & if \quad m_j - \sigma_j < x_i \le m_j \\ \dfrac{-x_i + m_j + \sigma_j}{\sigma_j} & if \quad m_j < x_i \le m_j + \sigma_j \end{cases} \tag{9}$$
$$i = 1, 2. \qquad j = 1, 2, \ldots, 6.$$

where $\mu_j(x_i)$ is the output of the *j*th node of the *i*th input variable; σ_j is the center's width of the triangle; m_j is the center of the triangle.

3. Probabilistic layer (layer 3): For the same reason in membership layer, another triangular function $f_p(\mu_j)$ is designed as the receptive field function and its equations are provided as:

$$P_k(\mu_j) = f_p(\mu_j) = \begin{cases} 0 & if \quad \mu_j \ge m_k + \sigma_k,\ \mu_j \le m_k - \sigma_k \\ \dfrac{\mu_j - m_k + \sigma_k}{\sigma_k} & if \quad m_k - \sigma_k < \mu_j \le m_k \\ \dfrac{-\mu_j + m_k + \sigma_k}{\sigma_k} & if \quad m_k < \mu_j \le m_k + \sigma_k \end{cases} \tag{10}$$
$$k = 1, 2, \ldots, 18$$

where $P_k(\mu_j)$ is the output of the *k*th node of the *j*th input variable; σ_k is the center's width of the triangle; m_k is the center of the triangle.

4. Rule layer (layer 4): In this layer, each node corresponds to a rule in the knowledge base. In the Mamdani inference, the node itself performs the product operation to obtain the inference set according to the rules as shown in (11). The probabilistic information is processed using the Bayes'

theorem [12] in consideration of the group of fuzzy grade being independent variables as shown in (12). Thus, the input and the output of this layer are described as:

$$\mu_l^I = \prod_j w_{jl}\mu_j \tag{11}$$

$$P_l^I = \prod_k w_{kl}P_k \tag{12}$$

$$\mu_l^O = \mu_l^I P_l^I \qquad l = 1, 2, \ldots, 9. \tag{13}$$

where P_l^I and μ_l^I are the input of rule layer; w_{kl} is the connective weight between the probabilistic layer and the rule layer which is set to be 1; w_{jl} is the connective weight between the membership layer and the rule layer, which is also set to be 1; μ_l^O is the output of the rule layer.

5. output layer (layer 5): In this layer, the input and the output of the node are obtained as:

$$y(N) = \Delta i = \sum_{l=1}^{9} w_l \mu_l^O \tag{14}$$

where $y(N) = \Delta i$ is the output of the PFNN; w_l is the connective weight between the rule layer and the output layer.

B. Online Learning Algorithm

According to the supervised learning algorithm, the parameter learning can be achieved by online regulate the connective weights between the output layer and rule layer, and the mean and standard deviation of the membership functions using the BP algorithm to minimize a given energy function. Hence, in order to describe the online learning algorithm of the PFNN, first the energy function E is defined as:

$$E = \frac{1}{2}(P_{inv}^* - P_{inv})^2 = \frac{1}{2}e^2 \tag{15}$$

Then, the update rules for the parameters in the PFNN are introduced as follows:

1. Layer 5: In this layer, the error term to be propagated is computed as:

$$\delta_o = -\frac{\partial E}{\partial y(N)} = -\frac{\partial E}{\partial P_{inv}}\frac{\partial P_{inv}}{\partial y(N)} \tag{16}$$

By using the chain rule, the connective weights are updated by the amount:

$$\Delta w_l = -\eta_1 \frac{\partial E}{\partial w_l} = -\eta_1 \frac{\partial E}{\partial y(N)}\frac{\partial y(N)}{\partial w_l} = \eta_1 \delta_o \mu_l^O \tag{17}$$

where the factor η_1 is the learning rate. The connective weight w_l is updated by the followings:

$$w_l(N+1) = w_l(N) + \Delta w_l \tag{18}$$

2. Layer 4: In this layer, the error terms to be propagated are described as:

$$\delta_l = -\frac{\partial E}{\partial \mu_l^O} = -\frac{\partial E}{\partial y(N)}\frac{\partial y(N)}{\partial \mu_l^O} = \delta_o w_l \tag{19}$$

3. layer 2: The error terms to be propagated are obtained by:

$$\delta_j = -\frac{\partial E}{\partial \mu_j} = -\frac{\partial E}{\partial y(N)}\frac{\partial y(N)}{\partial \mu_l^O}\frac{\partial \mu_l^O}{\partial \mu_l^I}\frac{\partial \mu_l^I}{\partial \mu_j} = \sum_l \delta_l P_l^I \tag{20}$$

By using of the chain rule, the update laws of center and center's width of the triangle are computed as follows:

$$\begin{aligned}\Delta m_j &= -\eta_2 \frac{\partial E}{\partial m_j} = -\eta_2 \frac{\partial E}{\partial y(N)}\frac{\partial y(N)}{\partial \mu_l^o}\frac{\partial \mu_l^o}{\partial \mu_l^I}\frac{\partial \mu_l^I}{\partial \mu_j}\frac{\partial \mu_j}{\partial m_j} \\ &= \begin{cases} -\eta_2 \delta_j \dfrac{1}{\sigma_j} & if \quad m_j - \sigma_j < x_i \le m_j \\ \eta_2 \delta_j \dfrac{1}{\sigma_j} & if \quad m_j < x_i \le m_j + \sigma_j \end{cases}\end{aligned} \tag{21}$$

$$\begin{aligned}\Delta \sigma_j &= -\eta_3 \frac{\partial E}{\partial \sigma_j} = -\eta_3 \frac{\partial E}{\partial y(N)}\frac{\partial y(N)}{\partial \mu_l^o}\frac{\partial \mu_l^o}{\partial \mu_l^I}\frac{\partial \mu_l^I}{\partial \mu_j}\frac{\partial \mu_j}{\partial \sigma_j} \\ &= \begin{cases} \eta_3 \delta_j \dfrac{m_j - x_i}{(\sigma_j)^2} & if \quad m_j - \sigma_j < x_i \le m_j \\ \eta_3 \delta_j \dfrac{x_i - m_j}{(\sigma_j)^2} & if \quad m_j < x_i \le m_j + \sigma_j \end{cases}\end{aligned} \tag{22}$$

where η_2 and η_3 are the learning rates. The center of the triangle m_j and center's width of the triangle σ_j are updated according to:

$$m_j(N+1) = m_j(N) + \Delta m_j \tag{23}$$

$$\sigma_j(N+1) = \sigma_j(N) + \Delta \sigma_j \tag{24}$$

The exact calculation of the sensitivity of the system $\partial E / \partial y(N)$ which is contained in $\partial P_{inv} / \partial y(N)$ and $\partial Q_{inv} / \partial y(N)$ cannot be determined due to the uncertainties of the plant dynamic such as parameter variations and external disturbances. To overcome this problem and to increase the online learning rate of the network parameters, the delta adaptation law is adopted as:

$$\delta_o \cong e(N) + A\dot{e}(N) \tag{25}$$

where A is a positive constant.

IV. Experimentation

The block diagram of the grid-connected power inverter system for the islanding detection method is provided in Fig. 4, where C_{dc}, V_{dc}, i_{dc} are capacitor, DC link voltage and current

respectively; L_f is inductor between the power inverter and utility power; i_{us}, i_{vs}, i_{ws} are the three-phase power inverter currents; V_{un}, V_{vn}, V_{wn} are the three-phase voltages of *RLC* load; T_a, T_b, T_c are the control signals of power inverter. The switch S1 represents the utility circuit breaker. When the S1 closes, the power inverter systems operate in grid-connected mode. On the other hand, when the S1 opens, the utility power is disconnected. The parallel *RLC* resonant load represents a local load, and the *RLC* resonant frequency is designed to 60 ± 0.1*Hz*. Moreover, when the utility frequency is 60*Hz*, the *RLC* resonant load represents a resistive load. If the utility power fails and the output power of the power inverter and the *RLC* load power are balanced, without effective islanding detection method, the output voltage and frequency of the power inverter will be maintained as same as the utility power resulting in the islanding phenomenon. Therefore, this test system can be applied to determine if the islanding detection method is valid.

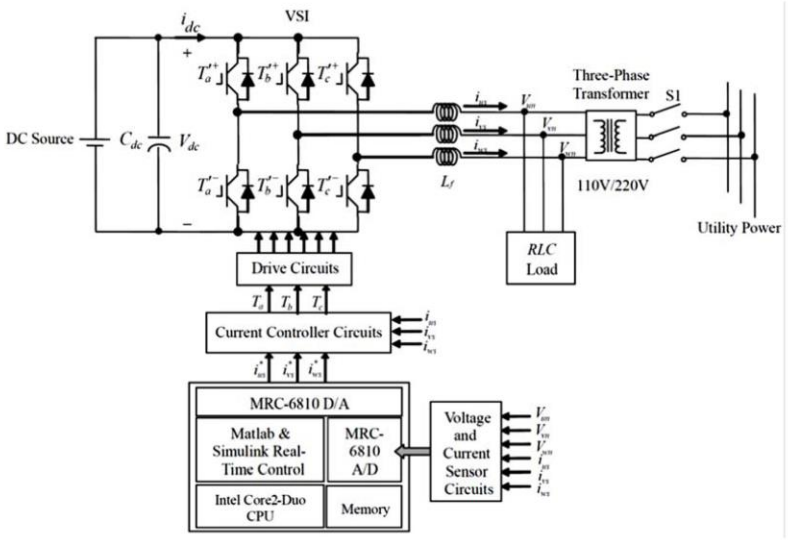

Fig. 4 Block diagram of the grid-connected power inverter system for islanding detection

In the experimentation, first, some experimental results using PI and PFNN controllers for the tracking control of the active and reactive power are demonstrated to show the control performance of the power inverter with the current injection disturbance. The experimental results of using PI controller for active power command from 0kW to 2kW and reactive power command set to be 0Var are shown in Fig. 5. In this study, the gains of the PI controller are obtained by trial and error in order to achieve good transient and steady-state control performance. The responses of active power and reactive power outputs of the power inverter are shown in Figs. 5 (a) and (b). Moreover, the experimental results using PFNN controllers for active power command from 0kW to 1kW and reactive power command set to be 0Var are shown in Fig. 6. The responses of active power and reactive power outputs of the power inverter are shown in Figs. 6 (a) and (b). From the experimental results, excellent tracking responses of both active power and reactive power can be obtained for the PFNN controller owing to the online training ability. Furthermore, the output active power and reactive power of the power inverter are not affected by the added disturbance signal. In addition, the robust control performance of the adopted PFNN controller at different operating conditions is obvious.

To verify the effectiveness of islanding detection, the utility frequency 60 Hz is designed to test the effectiveness of the proposed active islanding detection method. When the S1 shown in Fig. 4 opens, the utility power is disconnected. Fig. 7 shows the experimental results of injection disturbance method using PI controller operated at 60 Hz. The responses of frequency at the terminal of the *RLC* load and the active power output are shown in Figs. 7 (a) and (b), where P_{inv}^{*} is set to be 2kW and Q_{inv}^{*} is set to be 0Var. The utility power is disconnected at the time 1s, and the power inverter continues to deliver active power to the *RLC* load until the time 1.75s. After 1.75s, the disturbance signal is large enough to drift the frequency to shift out of the IEEE1547 scope. From Fig. 7 (a), the total time for the PI controlled power inverter stop delivering power is about 0.75s, which meets the IEEE1547 regulations (2s). Moreover, the experimental results of injection disturbance method using PFNN controller are provided in Fig. 8. The responses of frequency at the terminal of the *RLC* load and the active power output are shown in Figs. 8 (a) and (b). From the experimental results shown in Figs. 8 (a)

and (b), the total time for the PFNN controlled power inverter stop delivering power is about 0.45s, which also meets the IEEE1547 regulations. Compared with the experimental results of the proposed islanding detection method using PI controller, the responses of the proposed islanding detection method using PFNN controller are faster due to the advantages of PFNN such as online learning and quick convergence. Thus, the proposed islanding detection method using PFNN controller has excellent performance for the islanding detection.

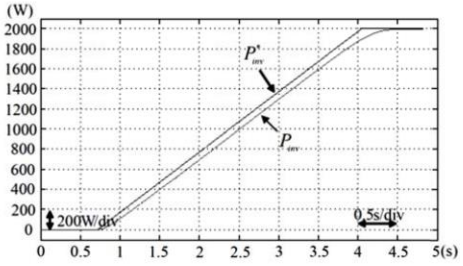

(a)

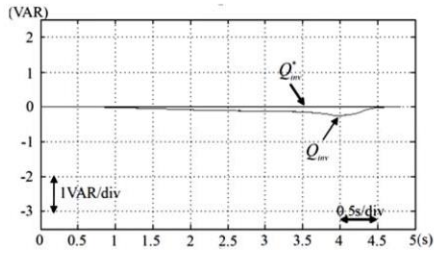

(b)

Fig. 5 Experimental results of PI controllers for tracking control, (a) responses of active power and active power command, (b) responses of reactive power and reactive power command

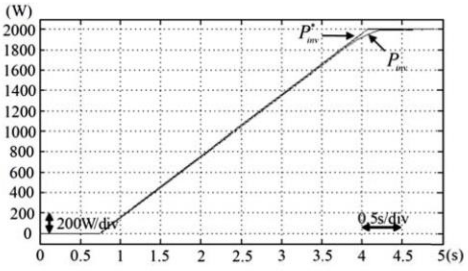

(a)

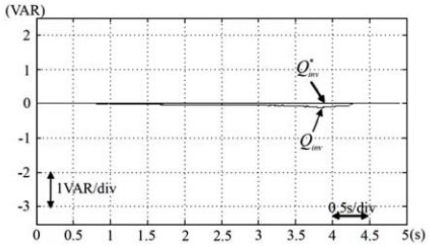

(b)

Fig. 6 Experimental results of PFNN controllers for tracking control, (a) responses of active power and active power command, (b) responses of reactive power and reactive power command

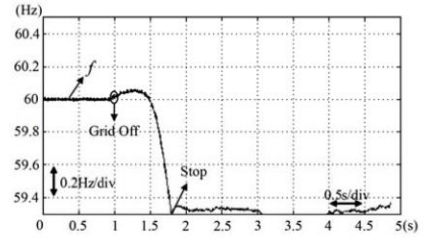

(a)

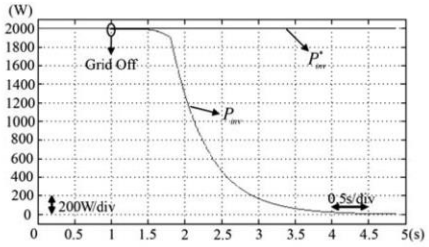

(b)

Fig. 7 Experimental results of PI controllers for proposed islanding detection, (a) frequency responses, (b) responses of active power and active power command

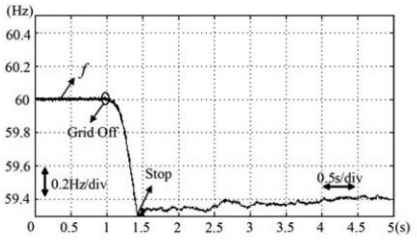

(a)

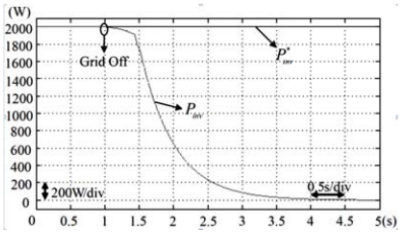

(b)

Fig. 8 Experimental results of PFNN controllers for proposed islanding detection, (a) frequency responses, (b) responses of active power and active power command

V. CONCLUSION

This study has successfully demonstrated the applications of the PFNN controllers on the power inverter for the tacking control of active power and reactive power outputs. Moreover, a novel islanding detection method has been successfully proposed. The proposed active islanding detection method is based on injecting a disturbance signal into the power inverter emulated the DG system through the *d*-axis current. Furthermore, the network structure and online learning algorithms of the adopted PFNN have all been described in detail. Finally, the proposed islanding detection method combined with the PFNN controller for active islanding detection has been successfully verified in the experimental results.

ACKNOWLEDGMENT

The author would like to acknowledge the financial support of the Ministry of Science and Technology of Taiwan through its grant MOST 103-2221-E-606-006.

REFERENCES

[1] M. Ciobotaru, V. Agelidis, and R. Teodorescu, "Accurate and less-disturbing active anti-islanding method based on PLL for grid-connected PV Inverters," in *2008 Proc. IEEE Power Electronics Specialists Conf.*, pp. 4569-4576.

[2] IEEE, Std. 1547, "IEEE standard for interconnecting distributed resources with electric power systems," 2003.

[3] UL 1741, "Inverters, converters, and controllers for use in independent power systems," 2002.

[4] IEEE, Std. 929-2000, "IEEE recommended practice for utility interface of photovoltaic (PV) systems," 2000.

[5] M. E. Ropp, M. Begovic, A. Rohatgi, "Analysis and performance assessment of the active frequency drift method of islanding prevention," *IEEE Trans. Energy Conversion*, vol. 14, no.3, pp. 810–816, Sep. 1999.

[6] H. Karimi, A. Yazdani, and R. Iravani, "Negative-sequence current injection for fast islanding detection of a distributed resource unit," *IEEE Trans. Power Electronics*, vol. 23, no. 1, pp. 298–307, Jan. 2008.

[7] B. Y. Bae, J. K. Jeong, J. H. Lee, and B. M. Han, "Islanding detection method for inverter-based distributed generation systems using a signal cross-correlation scheme," *J. Power Electron*ics, vol. 10, no. 6, pp. 762–768, 2010.

[8] T. T. Ma, "Novel voltage stability constrained positive feedback anti-islanding algorithms for the inverter-based distributed generator systems," *IET Renewable Power Generation*, vol. 4, no. 2, pp. 176-185, March, 2010.

[9] F. Wang, and Z. Mi, "Passive islanding detection method for grid connected PV system," in *2009 Proc. Int. Conf. on Industrial and Information Systems*, pp. 409-412

[10] Y. Gao, and M. J. Er, "An intelligent adaptive control scheme for postsurgical blood pressure regulation," *IEEE Trans. Neural Networks,* vol. 16, no. 2, pp. 475-483, March, 2005.

[11] F. J. Lin, H. J. Shieh, P. K. Huang, and L. T. Teng, "Adaptive control with hysteresis estimation and compensation using RFNN for piezo-actuator," *IEEE Trans. Ultrasonics, Ferroelectrics, and Frequency Control*, vol. 53, no. 9, pp. 1649-1661, Sept. 2006.

[12] M. Tripathy, R. P. Maheshwari, and H. K. Verma, "Application of probabilistic neural network for differential relaying of power ransformer," *IET Generation, Transmission and Distribution*, vol. 1, no. 2, pp. 218–222, March, 2007.

[13] N. Perera, and A. D. Rajapakse, "Recognition of fault transients using a probabilistic neural-network classifier," *IEEE Trans. Power Delivery*, vol. 1, no. 26, pp. 410-419, Jan., 2011.

[14] M. Tripathy, R. P.Maheshwari, and H. K. Verma, "Power transformer differential protection based on optimal probabilistic neural network," *IEEE Trans. Power Delivery,* vol. 25, no. 1, pp. 102-112, Jan., 2010.

[15] H. X. Li, and Z. Liu, "A probabilistic neural-fuzzy learning system for stochastic modeling," *IEEE Trans. Fuzzy Systems,* vol. 16, no. 4, pp. 898-908, Aug., 2008.

[16] F. J. Lin, Y. S. Huang, K. H. Tan, Z. H. Lu, and Y. R. Chang, "Intelligent-controlled doubly fed induction generator system using PFNN," *Neural Computing and Applications*, vol. 22, no. 7-8, pp. 1695-1712, 2013.

[17] A. Yafaoui, B. Wu, and S. Kouro, "Improved active frequency drift anti-islanding detection method for grid connected photovoltaic systems," *IEEE Transactions on Power Electronics,* vol. 27, no. 5. pp. 2367-2375, May, 2012.

K. H. Tan received the B.S., M.S., and Ph.D. degrees in electrical and electronic engineering from Chung Cheng Institute of Technology (CCIT), National Defense University (NDU), Taiwan, ROC in 2002, 2007 and 2013, respectively. He has been a member of the faculty at CCIT, where he is currently an assistant professor in the Department of Electrical and Electronic Engineering. His teaching and research interests include power electronics, microgrid system and intelligent control.

C. C. Hu received the B.S. and M.S. degrees in Electrical and Electronic Engineering from Chung-Cheng Institute of Technology, Taiwan in 2002, and 2007, respectively. He was received the Ph.D. degree in Electrical Engineering from National Central University, Taiwan in 2015. He has been a deputy engineer of the System Manufacturing Center at National Chung-Shan Institute of Science and Technology, and his research interests include nanophotonics, electromagnetic field simulation, near-field optics and plasmonics.

C. W. Lan was born in Tainan, Taiwan, 1981. He received the B.S., M.S. and Ph.D. degrees from the Department of Electrical and Electronic Engineering, and the School of Defense Science, Chung Cheng Institute of Technology, National Defense University, Taoyuan, Taiwan, in 2003, 2006, and 2013, respectively. He is currently an Assistant Professor of the Department of Electrical and Electronic Engineering of Chung Cheng Institute of Technology, National Defense University. His current research interests include humanoid robot, computer vision, and remote control.

S. S. Lin received the B.S. degree and the M.S. degree from the Department of Electrical Engineering, Chung Cheng Institute of Technology (CCIT) in 1997 and 2003 respectively, and the Ph.D. degree from CCIT, National Defense University (NDU) in 2010. Currently, he is an associate professor of the Department of Electrical and Electronic Engineering, CCIT, NDU, Taoyuan, Taiwan. His current research interests include Web-based automation, RFID applications, WSN-based control and monitoring applications, power monitoring systems and microprocessor systems.

T. J. Chang received the B.S., M.S., and Ph.D. degrees in electrical and electronic engineering from Chung Cheng Institute of Technology (CCIT), National Defense University (NDU), Taiwan, ROC in 1993, 2001 and 2008, respectively. He has been a member of the faculty at CCIT, where he is currently an assistant professor in the Department of Electrical and Electronic Engineering. His teaching and research interests include operating system, information security, data structure, computer network.